The International Journal of Advanced Manufacturing Technology (2018) 96:4353–4366
https://doi.org/10.1007/s00170-018-1902-4

ORIGINAL ARTICLE

Analysis of the metallography parameters and residual stress induced when producing bolt holes in Inconel 718 alloy

Marek Vrabeľ[1] · Martin Eckstein[2] · Ildikó Maňková[1]

Received: 14 November 2017 / Accepted: 14 March 2018 / Published online: 25 March 2018

Abstract
Inconel 718 is a structural material used to produce highly stressed rotating aero-engine components. Such components have to meet the most exacting requirements in terms of reliability and component service life. Bolt holes in rotating turbine and compressor discs are among the most highly stressed geometric features of jet engines. In-flight failure of these bolt holes may, in fact, result in the loss of the aircraft and imperilment of human lives. For this reason, the quality and reliability of hole-making are of utmost importance. The integrity and reliability of the machined engine component are the sole factors for which all efforts are taken for system of design, material selection, manufacturing and inspection of these rotating aero-engine components. This paper aims to contribute towards a safer production of bolt holes in highly stressed turbine discs made from nickel based super-alloy, which acts as a linking sequence between microstructural surface integrity and descriptive residual stress parameters. The magnitude of the residual stress was determined by means of combining two various methods, namely surface stress measurement by X-ray diffraction and hole-drilling, to achieve residual stress in the profile depth.

Keywords Drilling · Reaming · Ni based alloy · Hole making · Residual stress · Microstructure

1 Introduction

Hole-making is one of the most common manufacturing processes in machining practice; it is also widely used to produce aero-engine components made from difficult-to-cut superalloys as Inconel 718. This nickel-based superalloy is the most popular choice of material used in aerospace applications and modern jet engines constituting about 75 and 50% of weight, respectively [1]. According to Herbert et al. [2], complex aero-engine parts demand the use of careful processing routes to ensure robust manufacture right from the forging to the finish cutting operation. In particular, the quality of hole features in the rotating parts must be carefully considered as they could become fatigue initiators. Traditional metal removal processes are applied for highly stressed bolt holes in rotating aero-engine parts, which is the subject matter of this paper. However, research in hole making so far has not been performed to the extent of other metal removal processes, such as turning [3], milling [4] or broaching [5]. Consequently, scientific literature about drilling of Inconel 718 is very limited [6–9].

The most highly stressed holes are the bolt holes in the flange or in the rim of the discs or holes in rotating air seals. Diameters of bolt holes in the flange of aero-engine turbine discs are usually between 5 and 10 mm [10] since the hole length-to-diameter ratio varies from 0.5 to 3. To limit the influence of the chip removal on the generated surface integrity, multi-step hole-making processes are applied. A typical machining sequence consists of a drilling process for twist drill removal of most of the workpiece material. This operation is followed by a second machining process. This process typically involves application of a reamer (special face-cutting finisher) as a finishing tool that removes an additional radial allowance from 0.10 to 0.25 mm per side.

In addition to dimensional compliance to the component drawing, this strategy ensures that the integrity of the finished hole is not disturbed by any detrimental effects resulting from pre-drilling. Moreover, hole-making in aero-engine parts is always completed by corner rounding process on the entry

✉ Marek Vrabeľ
marek.vrabel@tuke.sk

[1] Faculty of Mechanical Engineering, Technical University of Košice, Mäsiarska 74, 040 01 Kosice, Slovakia

[2] MTU AeroEngines Munich, Dachauer Strasse 665, 809905 Munich, Germany

and on the exit of the hole. This is predominantly performed by circular milling process to create a defined radius within a range of 0.4 to 0.9 mm. This operation is followed by a brushing process with abrasive fibres, also called 'butterfly polish', which is essentially polishing with a rotating emery cloth, to remove microburrs.

To completely understand the impact of metal removal processes on the surface integrity (SI) of the machined parts, aero-engine manufacturers need to know the distribution of residual stress (RS) before and after any machining operation. RS can be defined as mechanical stresses that remain in the material or in the workpiece after the original cause for these stresses have been removed. RS exists in any elastic solid body in the absence of or in addition to the stresses caused by an external load. For example, it arises from deformation during cold working, in welding, during changes in volume due to thermal expansion, and also during manufacturing and processing of materials. RS is caused by heterogeneous plastic deformations, thermal contractions and phase transformations [11]. Today, the industry uses analytical methods for evaluating RS to optimize heat treatment processes [12, 13] and for metal forming [14]. Some examples are available in literature that describe how metal removal processes predominantly grinding, but to certain extent also turning, milling and drilling, affect RS. Adam, P in his published work [15], gives an outline of how processes, such as turning, milling and grinding, affect surface properties and residual stress when producing jet engine components. It has been shown that turning with cubic boron nitride (CBN) inserts within a cutting speed range of 250–400 m/min generates compressive stress, which contributes to the extension of the life cycle to failure (LCF) of the engine parts [10, 16]. Adam, P also introduced depth profiles of the RS in a case of turning Inconel 718 by combining X-ray diffraction with the hole drilling method [15]. It was concluded that the turning Inconel with both reinforced ceramics and CBN generate significantly higher level of RS compared to sintered carbide. However, far less information has been published about the influence of the drilling process on the RS for holes as this is difficult to investigate. The access to the bore is limited for the simultaneous application of both the X-ray diffraction and the hole drilling method. Liu, CR [17] described an approach to optimize single-step drilling operations towards maximum fatigue life when using RS measurements as an indicator of process excellence. Data published by Eckstein, M for machined bolt holes in rotating jet engine components showed that RS profiles were ascertained with a combination of the X-ray diffraction method and the hole-drilling method [18]. The surface RS was measured with X-ray diffraction, and the RS depth profile below was measured with the hole-drilling method. Data was obtained for drilled as well as for finished surfaces, by the reaming operation. All data obtained were measured towards the end of the bolt hole (drill or reamer exit from the machined hole). In scientific literature, there is no definition of a 'worst case location' referred to RS. However, it is known that worn tools produce an overall higher level of plastic deformations than the new ones for instance, in a case demonstrated by Wessels for drilling Inconel 718 with twist drills and gun-drills [19]. Farid et al. [20] investigated the microstructural properties of drilled holes in Inconel 718 samples. Similarly, phenomena, such as white layer, bended grain boundaries and plastic deformations, occurring due to the cutting path, have been observed. It was found that increased flank wear and increase in cutting speed increase white layer formation. Excellent research by Sharman [9] regarding the drilling and hole making of Inconel 718 with respect to its surface integrity and tool life suggests that drilled holes are insufficient to meet the standards required by the aerospace industry. Such research has confirmed that the holes produced by reaming or mill boring exhibit lower surface roughness and minimal microstructural deformation, and the white layer produced through the drilling operation does not occur. Three possible mechanisms have been mentioned in the literature [2, 21] with relation to the formation of a white layer during the machining processes: (i) a phase transformation owing to rapid heating and quenching, (ii) severe plastic deformation creating a fine grain structure and (iii) a chemical reaction of the material with the environment, forming an oxide layer. Kwong et al. [22] examined the hole making of a Ni-based superalloy in terms of subsurface damage and residual stress. Their findings showed that the subsurface material deformation of a drilled hole is more significant in the hoop direction than in the axial direction. Ucak and Cicek [23] studied the effects of various cooling/lubrication conditions (dry, wet and cryogenic) in the drilling of Inconel 718 using solid carbide drills. Their quality was assessed through a comparison of the cutting force and torque, cutting temperature, surface roughness, hole diameter and roundness errors, burr formation, microstructural examination, microhardness and tool wear. When machining under wet conditions, a reduced thickness of the plastic deformation was observed in comparison to under dry conditions. Beer et al. [24] presented the possibility to reduce the heat load generated in drilling Inconel 718 through the modification of the solid carbide drill geometry; a modified geometry increased the tool life by about 50%. Through abusive drilling, Herbert et al. [25] observed that the white layer is similar to the bulk material but has a very fine grain size. Dutilh et al. [26] identified two types of distorted layer depending on the depth of the hole produced in the drilling of nickel alloy, Udimet 720.

Based on scientific literature, nothing is known about how the process of drilling produces the above-mentioned phenomena in the surface layer. Furthermore, nothing is known about how these phenomena, revealed by metallography of the surface layer, have their effects on the fatigue life of Ni-based superalloys. The dilemma of this question is that,

for example, plastic deformation, which occurs during machining, results both in cold work and in residual stress. Hardness and tensile strength are increased with the degree of cold work, while ductility and impact values are reduced. In addition, aero-engine components are exposed to high temperatures, and high operational stress. Thus, failure of the aero-engine components may be due to the super positioning of all the above-mentioned influencing factors. In retrospect, it is hard to define the extent to which the machining process alone has contributed to failure. Despite these uncertainties, aero-engine manufacturers consider microstructural evaluations as a vital step in determining process/product quality and/or to evaluate why a material or workpiece has failed. Taken together, it can be pointed out that the microstructural evaluation and residual stress measurements are key elements in the dataset of surface integrity for aero-engine components. The assessment of this data, according to specifications of engine maker, provides meaningful insights for process excellence. Besides one publication from Eckstein, M [18], no other published data was found for the cutting conditions applied, in drilling, and the subsequent finishing of highly stressed bolt holes, in turbine discs made from Inconel 718.

A two-step manufacturing hole-making process within the dimensions of bolt holes in turbine discs is the subject of this paper. Machining sequence consisting of drilling with a twist drill followed by the finishing operation with a reamer is used to investigate residual stress and microstructural changes on the surface as well as subsurface area. The present work, moreover, focuses on the study of possible correlation between descriptive parameters of residual stress and metallography by applying statistical methods for data analyses.

2 Materials and methods

2.1 Materials

A forging made of Inconel 718 (17.0% C, 50% Ni, 2.80% Mo, 4.75% Nb + Ta, 0.65% Ti, and 0.20% Al), a genuine turbine disc, was used to perform the machining experiments. Figure 1a shows a semi-finished shape to machine final turbine disc forging with a diameter of ~ 600 mm; the forged pieces were heat treated to achieve microstructure homogeneity. Heat treatment involved processes of solution annealing at 954 °C/1 h, with air cooling, precipitation hardening and ageing at 718 °C/8 h, rapid cooling to 621 °C/8 h and air cooling. Resultant hardness of the heat treated material was within the range of 410–435 HV (~ 42–45 HRc).

Heat treated forgings were machined with face turning to obtain a shape of flat discs with uniform thickness of 22 mm. CoroTurn style tungsten carbide inserts with a multi-layer $TiCN/Al_2O_3/TiN$ coating (ISO code CMT 09 T3 08-MF S05F, clearance angle 7°, tool nose radius 0.8 mm) were used

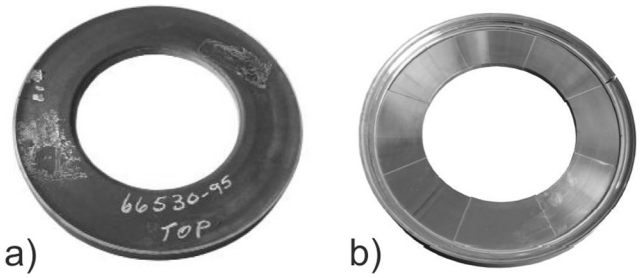

Fig. 1 Materials used in machining experiments. **a** Shape of a forging. **b** A machined forging sliced into eight parts with water jet cutting

to machine the forgings (cutting speed 75 m/min, depth of cut 0.7 mm, feed per rev 0.10 mm, cutting fluid 5% solution of semi-synthetic emulsion, flow rate 30 l/min, fluid supply 5 bars). Cutting inserts were mounted in a Sandvik Coromant tool holder with a designation QS-SCLCL 2525 09C. The rationale of applying such a tool nose radius (relatively small) was to avoid a thinning of chip: thinning effect is expected to reduce the transfer of heat away from the cutting edge and results to deeper thermally affected region beneath the workpiece surface. Higher cutting speed (75 m/min) was employed during test samples preparation to prevent of producing lower peak surface tensile stresses [31]. Compressive stress is preferred for contributing to an extension of LCF life on jet engine components as pointed out in [10, 16]. To facilitate subsequent machining experiments (drilling and reaming), water jet cutting was used to slice machined workpieces into eight segments shown in Fig. 1b). A workpiece segment made of flat discs and of a specific shape, as shown in Fig. 2, was used to investigate the machining operations in making bolt holes, drilling and reaming.

2.2 Machine tools, metal cutting tools and cutting conditions

All experiments were performed at MTU Munich, Germany. A Mikron UCP1050 five-axis machining centre with a Siemens Sinumerik 840D controller (spindle power 28 kW, maximum rotation speed 15.000 rpm) was used to machine bolt holes in the turbine discs. This machine tool allowed two ways of coolant supply: (i) internal coolant supply in the machine tool spindle and (ii) coolant supply through external nozzles. Tool edge cooling was applicable in both directions simultaneously (maximum coolant flow rate was 25 l/min and maximum coolant pressure was 60 bars).

Figure 3 shows the solid carbide cutting tools made by grinding. The drilling tools were ground from EMT210 Extramet rounded bars with two coolant holes (average grain size 0.8 μm, transverse rupture strength > 4300 N/mm^2, fracture toughness 10 MPa $m^{1/2}$), while reamers were made of the rounded bars without cooling holes (solid bar). Both types of cutting tools were applied without coating. The rationale of such a choice resulted from a study by Ucak and Cicek [23],

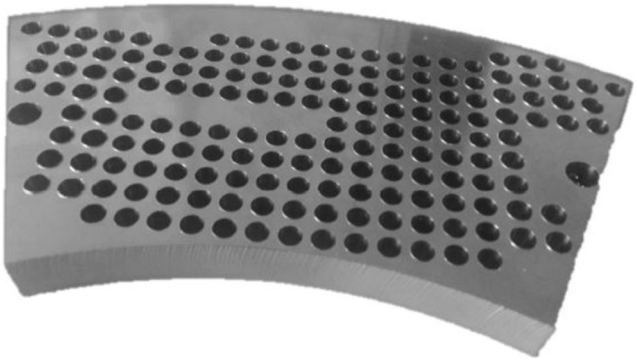

Fig. 2 Shape of workpiece segment made of flat disc to perform a series of drilling tests

who found that uncoated drills have a higher thermal conductivity and sharper cutting edges owing to the absence of a coating material and therefore generate less heat, which can negatively affect the microstructural changes in the machined layer. The tool diameter of the twist drill and the reamer was 8.2 and 8.5 mm, respectively. To clamp the cutting tools, hydraulic expansion chucks HSK63 were used for all experiments. Table 1 summarizes the geometric data about these cutting tools.

Table 2 shows a review of the machining parameters, such as cutting conditions, machining sequence and coolant supply, which were applied within a range of the actual capacity of bolt holes in turbine disc production.

Two tool life criteria were defined; the flank wear(i) VB_{max} = 200 μm, for machining of the bolt hole with twist drill, and (ii) VB_{max} = 150 μm, for reaming the operation of finishing of the bolt hole surface, respectively. Within all machining operations, a coolant was supplied to the cutting zone. During the drilling operation, the coolant medium was supplied both by means of high pressure through the spindle as well as additional flooding. During the finishing operation, the reamer was cooled down by means of flooding only. The cutting oil Castrol Honilo 971 CF was used as a coolant medium in both hole-making operations, which is during drilling and reaming.

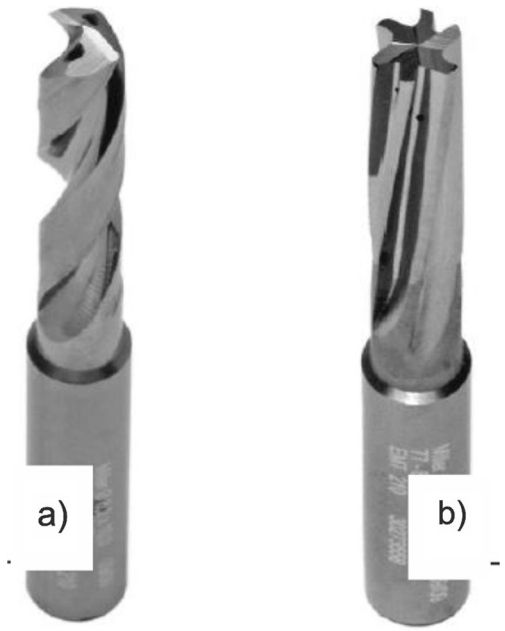

Fig. 3 Uncoated solid carbide cutting tools made from EMT210 Extramet rounded bars. **a** A twist drill to produce rough bolt hole. **b** A reamer to finish the final shape of the bolt hole

2.3 Metallography and its parameters

Two magnifications of × 500 and × 1000 were applied in metallographic analysis. Figure 4 shows that there are two ways of preparing samples to analyse the effect of machining on deformation below the machined surface. The first method is a metallographic sample made of an axial cross section of the bolt hole (Fig. 4a) being produced as shown in Fig. 4b. The second method is prepared from a radial cross section of the machined hole near the tool exit (~ 3 mm from the hole bottom) as shown in Fig. 4c. The rationale for this way of sampling was based on the specifications of the engine manufacturers who defined an axial sample of a hole in the direction of the cutting tool feed, while the radial cutup referred to the hole cross-section that was perpendicular to the feed direction. Axial cuts showed only projection of the grains that were deformed and squeezed along the feed direction. However, the overall level of plastic deformation was not very significant in this case. Therefore, modifications of material structure are difficult to detect in their full extent. In contrast, this type of cutup simply allows to screen the hole over the full length and identify local anomalies. Due to their nature, the radial cutups can only be made in discrete locations along the feed direction. Cutups include only local information that may differ a few microns beneath or above this cutting position. For all investigations, one has to consider that the metallographic results depend on the exact location within the hole length and the orientation of the sample relative to the cutting direction for microstructural visual inspection. Sharman et al. [9] in machining of Inconel 718 concluded that the typical microstructural damage consists of grain boundaries deformed in the direction of cutting. Therefore, if not indicated differently, data from radial cutups at the tool exit were considered to be a part of metallographic analysis. Electro-discharge machining (EDM) was used to take metallographic samples from a location where the edge of the tool left the machined surface creating a cutting tool exit. Two kinds of samples were studied: first, samples were taken after machining with sharp (new) tool edges, and second, samples were taken after tool edges achieved their wear criteria mentioned above, which was the last hole before tool change.

All the cutups from drilling and reaming process were embedded into bakelite to prepare metallographic samples. SiC grinding, diamond polishing and microstructure revealing were done by means of the Inco718 Etchant.

Table 1 Geometric data of the solid carbide cutting tools made from EMT210 Extramet rounded bars

Cutting tool data	Unit	Twist drill	Reamer
Tool diameter	[mm]	8.2	8.5
Core diameter	[mm]	2.9	4.4
Tool length	[mm]	89	97
Flute length	[mm]	48	50
Number of flutes	[–]	2	6
Tool flank	[°]	10	12
Tool rake	[°]	8	6
Helix angle	[°]	30	18
Margin width	[mm]	0.2	not applicable
Tool edge micro geometry	[μm]	brushed 10-15 μm	as ground
Number of coolant holes and their location	[–]	2: tool flank	6: flute

Microstructural evaluation on test samples was performed for different purposes [27, 28]. In the context of this paper, metallography was a means of evaluating how the process of bolt hole making left its impact on the surface layer below the machined surface. Four descriptive parameters listed in Table 3 were developed to assess such an impact, while Fig. 5 shows an example of how the descriptive parameters were measured and identified.

It must be noticed that aero-engine manufacturers provide limits for the allowable extent of microstructural changes below the machined surface or machined surface defects initiated by the machining process. Such limits, however, are based on both experience from failure analysis and on results of the specimen tested under the conditions of a flight emission. This means that each original equipment manufacturer (OEM) of the aero-engine components defines such limits according to his customized specifications. Consequently, we believe that the chosen manufacturing methods and their sequence are capable of providing the fundamental data for the accepted standards being defined by the standards of the OEM.

As a preliminary metallographic analysis shown in Fig. 5, there is a huge change in the revealed microstructure below the machined surface that interferes not only with the immediate surface layer, but also with the individual microstructure grains. In fact, the descriptive parameters from Table 3 clearly point out the deformation inhomogeneity below the machined surface, a fact associated with residual stress.

2.4 Residual stress parameters and measuring

All residual stress measurements were obtained at MTU Aero Engines AG. The X-ray diffraction unit shown in Fig. 6 was used to identify the residual stress directly on the machined surface. Stepwise removal by etching and hole drilling method shown in Fig. 7 allowed measurement of the residual stress below the machined surface (depth profile of RS).

Residual surface stress was determined by means of X-ray diffraction. Using MnKα radiation, the {311} lattice planes at $2\theta = 151°$ were measured in accordance with the sin2ψ method. Therefore, the X-ray elastic constants E{311} = 191 GPa and v{311} = 0.29 were used. The applied software was STRESSTECH version 1.22.10. The residual stress depth profiles were recorded with the hole-drilling method in increments of 25 μm from the machined surface while the hole

Table 2 Machining parameters used in experiments

Machining parameters	Unit	Twist drill: diameter 8.2 mm	Reamer: diameter 8.5 mm
Radial depth of cut	[mm]	4.1	0.15
Cutting speed	[m/min]	20	30
Length-to-diameter ratio	[–]	~2.6	~2.6
Feed per tooth	[mm]	0.035	0.025
Type of cooling	[–]	Inner coolant supply and flooding	Flooding only
Coolant pressure	[bar]	45 (inner coolant supply) 10 (flooding)	10 (flooding)
Coolant volume rate	[l/min]	12	15
Number of holes per tool per machining pass	[–]	24	30

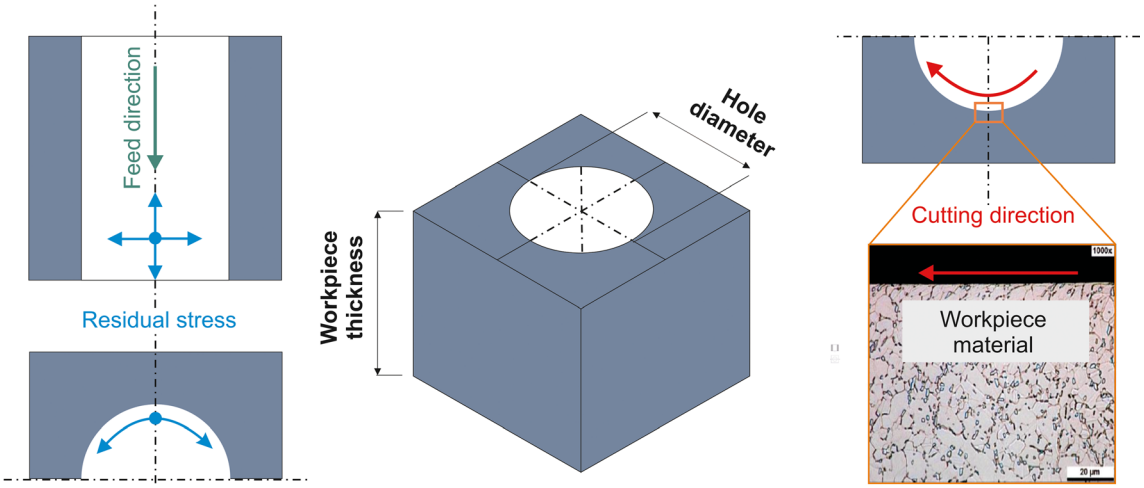

Fig. 4 Procedure of sample preparation for metallographic analysis and RS measurement

diameter was about 0.6 mm. The holes were drilled with a very gentle circular milling method. The tooling applied was air-driven milling/drilling equipment selected at MTU-AE, a device that can be compared to a dentist drill running at ~ 100,000 rpm. To ensure that the location for metallographic studies matches the position of residual stress, the holes were cut into half following the feed direction. The first half was inspected by metallography; the second half was subjected to residual stress measurements. All measurements were taken as close as possible to the exit in the known direction of the main stress, i.e. the direction of cutting (hoop direction) and the feed direction (axial direction) (see Fig. 4a).

3 Results and discussion

3.1 Metallographic analysis

The cutups shown in Fig. 8a, b were taken radial to the feed direction when drilling at the position of the tool edge exit from the machined hole. These cutups give evidence of how two different tool wear stages affect the machined surface and the subsurface layer. Figure 8a refers to the initial wear stage of VB_{max} at about 60 μm indicating a tiny microstructure protraction and plastic deformation. The machined surface of the bolt hole shown in Fig. 8b results from worn tool at $VB_{max} \approx 200$ μm. It is evident that the extent and the depth of plastic deformation and the degree of grain boundary distortion are significantly greater due to removal with a worn tool edge. This fact, however, concurs with all the experiences and expectations, even those with other materials and even with other kinds of metal removal process [29]. An almost identical phenomenon was observed and described in [20], which explained that chips produced during drilling are entrapped between the flute margins and the hole wall. These chips are extruded between the flute margins and the hole wall as the drill rotates and become pressure-welded to the workpiece surface, forming a white layer through the incipient melting and severe plastic deformation. This process continues as the drill is fed down the hole and as it is retracted. Moreover, the worn cutting tool increases the contact area of the tool workpiece and generates higher cutting as well as friction forces, which have a direct impact on the grain boundary deformation owing to a greater amount of rubbing of the workpiece surface. The effects of smearing when drilling using a worn tool and its undesirable influence, which have led to a premature service failure of the components in the aerospace industry,

Table 3 Metallography criteria parameters

No.	Abbreviation	Criteria or descriptive parameters	Unit
1	d_{int}	Severe plastic deformation	[μm]
2	d_{mod}	Moderate plastic deformation	[μm]
3	d_{sl}	Slip lines	[μm]
4	d_{wel}	White etching layer	[μm]

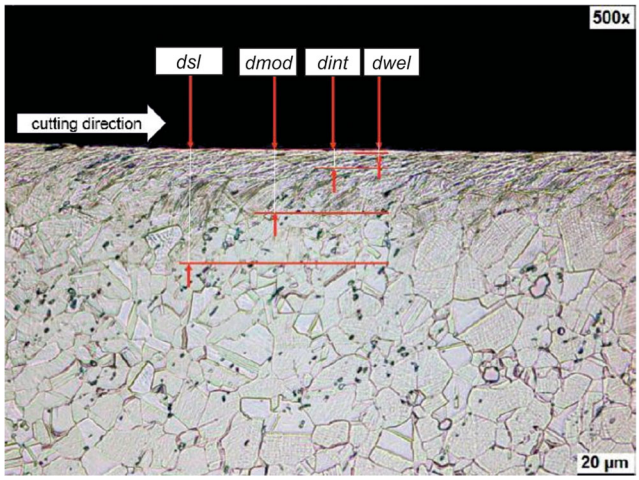

Fig. 5 Descriptive parameters for metallography analysis

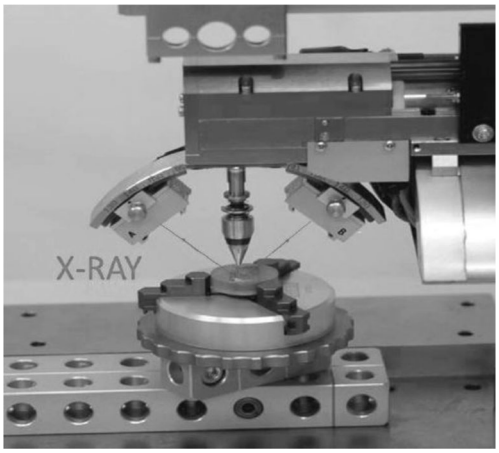

Fig. 6 X-ray diffraction unit for RS measurement

were confirmed in [9]. The authors also observed that microstructural damage to the subsurface in all of the drilled holes consists of deformed grain boundaries in the direction of the cutting, as well as a discontinuous white layer of up to 10 μm in thickness. The authors also confirmed that an uncoated cutting tool generates a lower cutting force, owing to a sharp cutting edge, in comparison to a coated tool (rounded cutting edge), thereby reducing the thickness of the affected zone.

A different influence of tool wear stages on machined surface integrity was proved in subsequent machining operation, namely reaming, and the comparison of such an influence is shown in Fig. 9. A significant feature of such an effect is that the initial tool wear stage $VB_{max} \approx 20$ μm leaves no evident grain boundary distortion and deformed layer as shown in Fig. 9a. Of note, the radial depth of the cut when reaming, which is nominally 150 μm, is far greater than the depth of the deformed surface layer resulting from drilling at ~20 μm. With respect to metallography, however, not necessarily with respect to the measured residual stress, the influence of drilling on the surface integrity and on the evolution of tool wear, by a work-hardened surface, appears to be small. Figure 9b clearly indicates tiny protraction of the deformed microstructure below the machined surface during machining with worn

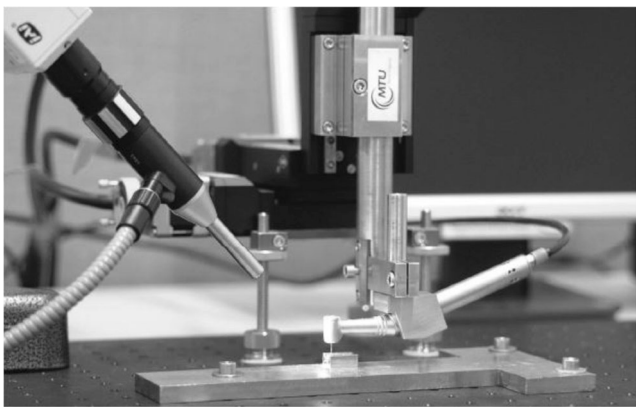

Fig. 7 Hole-drilling method

tool at $VB_{max} \approx 130$ μm. When reaming the bolt holes used in aerospace components, the contact length between the cutting edge and the machined surface should be considered. To preserve the sharpness of the cutting edge, a double relief of the cutting teeth was applied to produce less friction between the cutting edges and the machined surface [30]. The authors concluded that twist drilling or reaming with a normal reamer lead to an overheating of the machined surface (white layer formation) and material dragging. However, the use of a double relief angle on special reamers can generate finished holes within the standards accepted by the aerospace industry.

In summary, the metallographic cutups performed within a range of verification tests do not reveal any material damage, such as cracks, continuous white layer, alloy depletion or extreme plastic deformation. It has been proved that the effect of the applied machining operations was within a known range of considered workpiece and machining operations and showed compatibility with data presented by Adam, P [15]. In contrast, it is not clear whether and how these facts have been addressed in previous scientific investigations, because most of the available data do not provide the exact conditions, including locations and directions of metallographic testing. Therefore, the obtained results with our experiments cannot be compared directly to the recent results from scientific literature in a simple way.

3.2 Residual stress

The essential results of the residual stress measurements are compiled in Figs. 10 and 11. Considering results from metallography (see Fig. 5), which show a workpiece structure with plastic deformations induced by the metal cutting process, it can be expected that the residual stress must, at least to a certain extent, also show compressive stress. To fulfil the equilibrium conditions, a zone of tensile stress in the samples can also be expected. This is confirmed by Sharman et al. [31] and Madariaga et al. [1] during the evaluation of residual stress in the orthogonal cutting of Inconel 718 superalloy. They confirmed that the stress profile is generally tensile at the workpiece surface followed by a gradual reduction with increasing depth beneath it (becoming compressive) till it reaches a near non-stress value.

Figure 10 shows a residual stress depth profile taken from a sample machined with a sharp twist drill. The maximum flank wear VB_{max} was less than 60 μm. The influence of the drilling process on the residual stress of the workpiece can be considered to be not very severe in this case. This statement is mainly based on the yield strength of Inconel 718 which, according to Alloy 718 material data sheet, is about $R_{0.2} = 1034$ MPa. Machined surface transmits a reduced tensile stress, whereas a range between ~190 and ~250 MPa represents equilibrium of the compressive stress in a zone from about ~25 to ~200 μm under the machined surface. The maximum

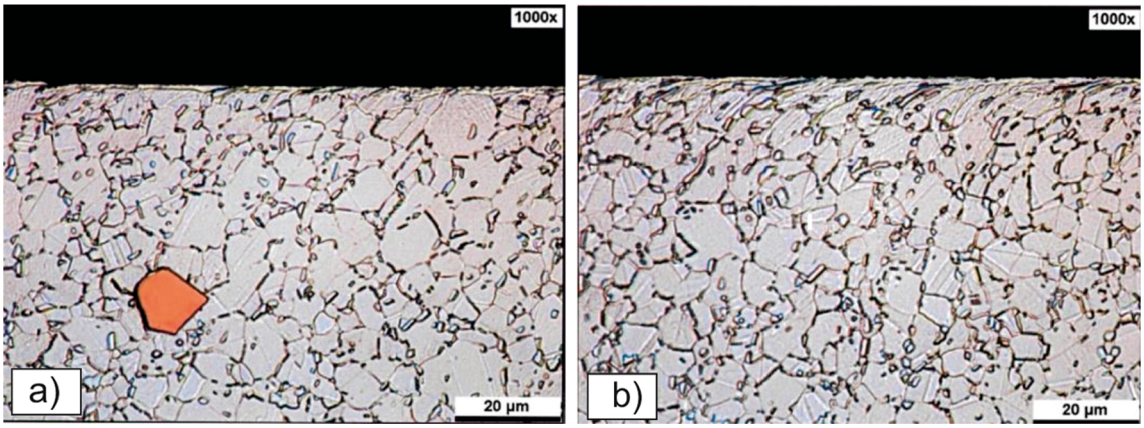

Fig. 8 A comparison of the tool wear effect on the machined surface when bolt hole drilling. **a** Initial wear $VB_{max} \approx 60$ μm. **b** Tool wear $VB_{max} \approx 200$ μm

compressive stress of about ~ 400 MPa was found obtained in a depth of 100 μm below the machined surface. The overall penetration depth of the residual stress could be measured up to ~ 200 μm under the machined surface. The main contribution to the compressive stress is caused by the full feed force of the drill, introducing high levels of plastic deformation into the workpiece along the axial direction. Because the thermal effects are expected to give rise to tensile stresses, the observed compressive stresses in the axial direction suggest that the mechanical straining behind the tool is more influential [22].

Figure 11 shows the effect of tool wear $VB_{max} \approx 200$ μm on the residual stress depth profile resulting from the same twist drill. As compared with the effect of the new tool edge shown in Fig. 10, the worn tool edge brings about two effects of how residual stress depth increases. First, the worn tool edge increases the tensile residual stress at machined surface itself by up to ~ 600 MPa, while the second effect is associated with an increase of the compressive stress in the depth of about ~ 125 μm below the machined surface. In addition, the maximum and the overall deformation depth move away from the workpiece surface. Because a blunt tool is incapable of efficiently removing material through cutting, more work is applied by the cutting edge in the feed direction of the drill, which leads to more plastic strain being retained on the surface, thus resulting in larger compressive residual stresses to greater depths [22]. A similar phenomenon in the turning of Inconel 718 was observed by Sharman et al. [32], who reported that, during all tests performed when cutting using a worn tool, the surface tensile stress increased dramatically. In addition, the stress beneath the surface layer became much more compressive and penetrated to a greater depth.

As previously mentioned in a text above, the finished holes represent the status of the drilling operation followed by a subsequent finishing process. For this reason, the penetration depth of the residual stress as it occurs after drilling is much more than the visible impact of machining in the metallographic analysis. It can be thus concluded that the allowance of 150 μm per side (radial depth of cut when reaming, see Table. 2) removed during the finishing process can eliminate the zone of tensile stress, by only half of the compressive stress below the machined surface. According to Kwong et al. [22], the removal of the material stock typically occurs within the range of 150–250 μm/radius when finishing critical engine components, and such a cut depth must ensure that the subsurface effects introduced by drilling are sufficiently

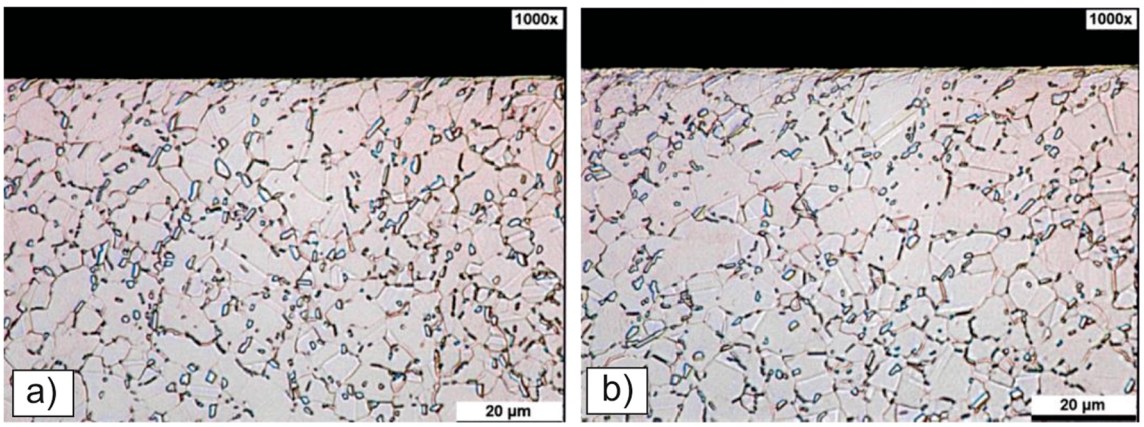

Fig. 9 A comparison of the tool wear effect on the machined surface during bolt hole reaming. **a** Initial wear $VB_{max} \approx 20$ μm. **b** Tool wear $VB_{max} \approx$ 130 μm

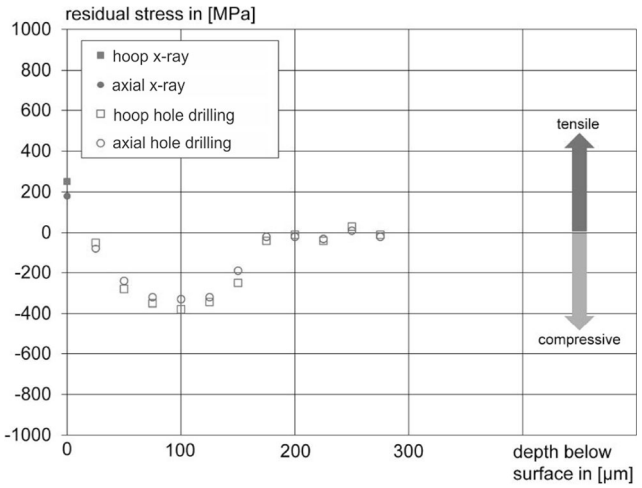

Fig. 10 Residual stress depth profile for drilling with a new tool, $VB_{max} \approx 60$ μm

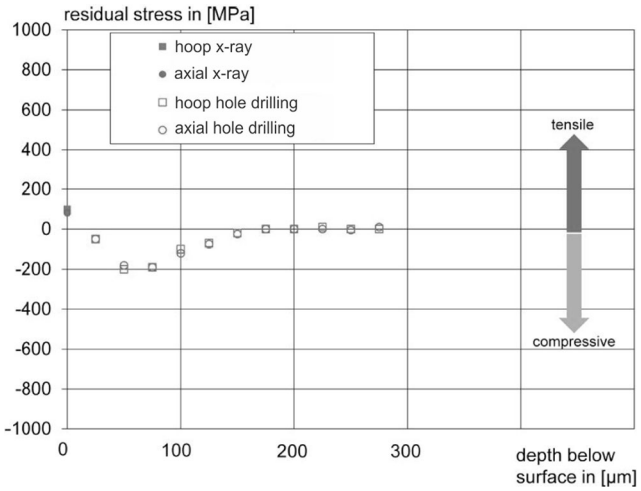

Fig. 12 Residual stress depth profile for reaming with a new tool, $VB_{max} \approx 20$ μm

removed. It is a reason to assert that the assessment of residual stress profile in the last surface layer (i.e. the surface layer after operation of reaming in this case) means a rather combined effect of all foregoing operations (operation of drilling as a roughing in this case). Unfortunately, there is a lack of available data in literature dealing with such a phenomenon for the operation sequence and the material applied within this paper. Therefore, we suggest that the residual stress depth profiles in Figs. 12 and 13 must be conceived as a superposition of the effect resulting from operation sequence in question, i.e. drilling and reaming. However, the general pattern of the residual stress profile, the tensile stress at the machined surface and the compressive stress below the machined surface did not change in comparison to the drilling method but changed according to its magnitude.

In the case of the new tool edge, the maximum compressive residual stress in operation of reaming was far lower, half of that of drilling on average, i.e. − 200 and − 400 MPa, respectively. However, this was not the case with a worn tool edge in reaming operation where VB_{max} was ~ 130 μm with residual stress of − 400 MPa.

The maximum compressive stress in Fig. 13 represents about 80% of the residual stress of drilling with worn tool edge as shown in Fig. 11. Further analysis involved reduction of the surface residual stress. Figures 12 and 13 show that tool edge wear in reaming produces quite different changes in tensile residual stress on the machined surface than that of drilling, at about 100 and 300%, respectively. However, such a result was expected due to higher tool wear limit of VB_{max} in the case of drilling (~ 25% higher compared to finishing operation with reamer). Sharman et al. stated that grain boundary distortion and overall plastic deformation were observed in machining with worn tools, regardless of the operating parameters being used, due to the higher cutting and frictional forces generated while cutting [29]. Flank wear VB reduces the clearance angle leading to greater rubbing of the workpiece surface and increases the tool/workpiece contact area.

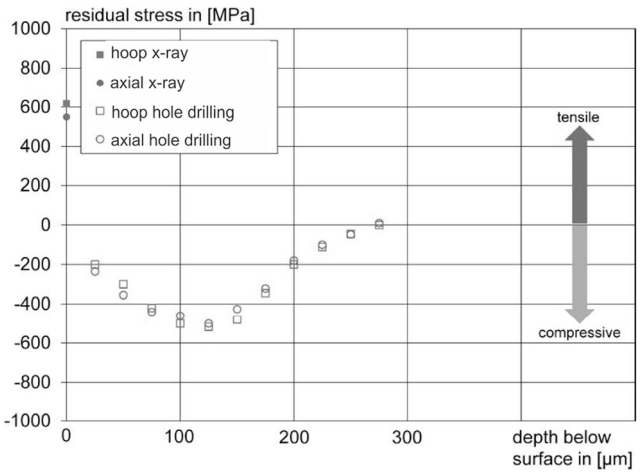

Fig. 11 Residual stress depth profile for drilling with a worn tool, $VB_{max} \approx 200$ μm

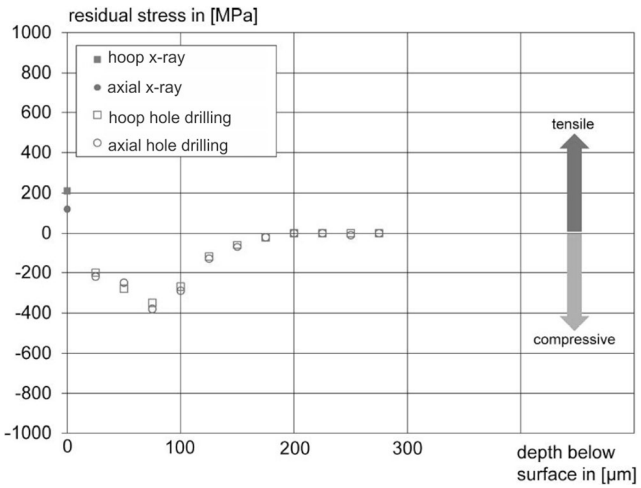

Fig. 13 Residual stress depth profile for reaming with a worn tool, $VB_{max} \approx 130$ μm

Table 4 Residual stress criteria parameters

No.	Abbreviation	Criteria or descriptive parameters	Unit
1	RS_{sur}	Residual stress on the surface	[MPa]
2	RS_{sub}	Max. compressive RS in the subsurface	[MPa]
3	RS_{dsu}	Penetration depth of max. compressive RS	[μm]
4	RS_{opd}	Overall penetration depth of residual stress	[μm]

3.3 Statistical analysis

The descriptive parameters of metallographic analysis shown in Fig. 5 were defined in the quality standards of the aero-engine manufacturers. These parameters denote a set of random data resulting from subsurface strain after applied machining operations. Moreover, residual stress data represent another major source of information about surface integrity of any machined component to the extent that a definite link between them and aforesaid descriptive parameters d_{int}, d_{mod}, d_{sl} and d_{wel} can be expected. This is why the overall residual stress profile can be also divided into a set of descriptive parameters. For effect of tool wear on residual stress shown in Figs. 10, 11, 12 and 13, residual stress description parameters, RS_{sur}, RS_{sub}, RS_{opd} and RS_{dsu} (see Table 4), can be displayed in the form of an average value (axial and hoop direction) as presented in Fig. 14.

The fact that the parameters in Fig. 5 are random data, an averaging of the residual stress data also justifies a way of finding out a relationship between residual stress and deformation of the surface layer, i.e. a correlation between them. A diagram in Fig. 15, a case of drilling, illustrates all data related to the drilling being drawn as their correlations. The first overview of possible correlations between descriptive parameters of metallography and residual stress is given by a matrix plot (correlogram), a complete array of possible scatterplots between defined datasets chosen for input and output (e.g. description parameters of metallography and residual stress). A principal correlation between metallographic parameters and the status of residual stress can be expected in a workpiece

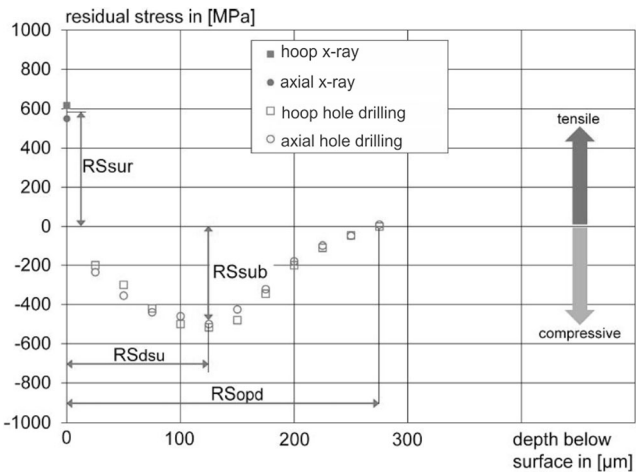

Fig. 14 Descriptive parameters of residual stress analysis

after machining at least to the extent that massive plastic deformation and compressive stress are directly linked. In contrast, it is hard to predict how residual stress performs with respect to cyclic life, especially if the component under consideration is exposed to high mechanical and thermal stress, which is typical for aero-engine components.

Based on the matrix plot illustrated above, it is clear that particularly the level of residual stress on the surface RS_{sur} seems to be a good source for data that are linked to the descriptive metallographic parameters. In one case of metallographic parameters resulting from drilling operation, it was found that d_{wel} formation is within a range from 0 to ~2 μm. These results are in contrast to those published by Sharman et al. [9], who observed that drilling Inconel 718 with TiAlN PVD coated WC-Co cutting tools having slightly different geometries, wherein a discontinuous white layer was found to be up to ~10 μm deep beneath the machined surface and was largely absent on the holes produced by reaming and mill boring. However, there are no available data about cutting tool micro geometry. Results from subsurface microstructure analysis are in compliance with those from the drilling employed tool with a sweeping curved cutting edge, especially from the perspective of d_{int}, which is within a range of ~5 to ~10 μm. Moreover, they also stated that the subsurface microstructural damage was observed in all the holes produced by drilling operation. Hood et al. [33] reported in their research related to twist drilling of Haynes 282 superalloy that surface/subsurface microstructural damage was generally confined to bent/deformed grain boundaries up to a depth of ~15 μm and discontinuous white layers up to ~6 μm thick from the workpiece surface. In summary, they confirmed that results obtained in drilling nickel alloy are comparable with results obtained when drilling Inconel 718 and RR1000. Calculating and comparing the level of determination are very helpful to receive a more detailed interpretation. Figure 16 outlines the range of determination coefficient (R^2) between 18 and 88% in a diagonal arrangement. The weakest correlation can be found between d_{wel} and RS_{opd}. It is comprehensible that the depth of intense plastic deformation d_{int} is linked most to the status of the tensile residual stress on the machined surface RS_{sur}. Since the radial allowance of workpiece material that is to be removed during operation of reaming is less than the overall penetration depth of residual stress generated by drilling, the formation of residual stress in a finished hole is created as a superposition of roughing and finishing.

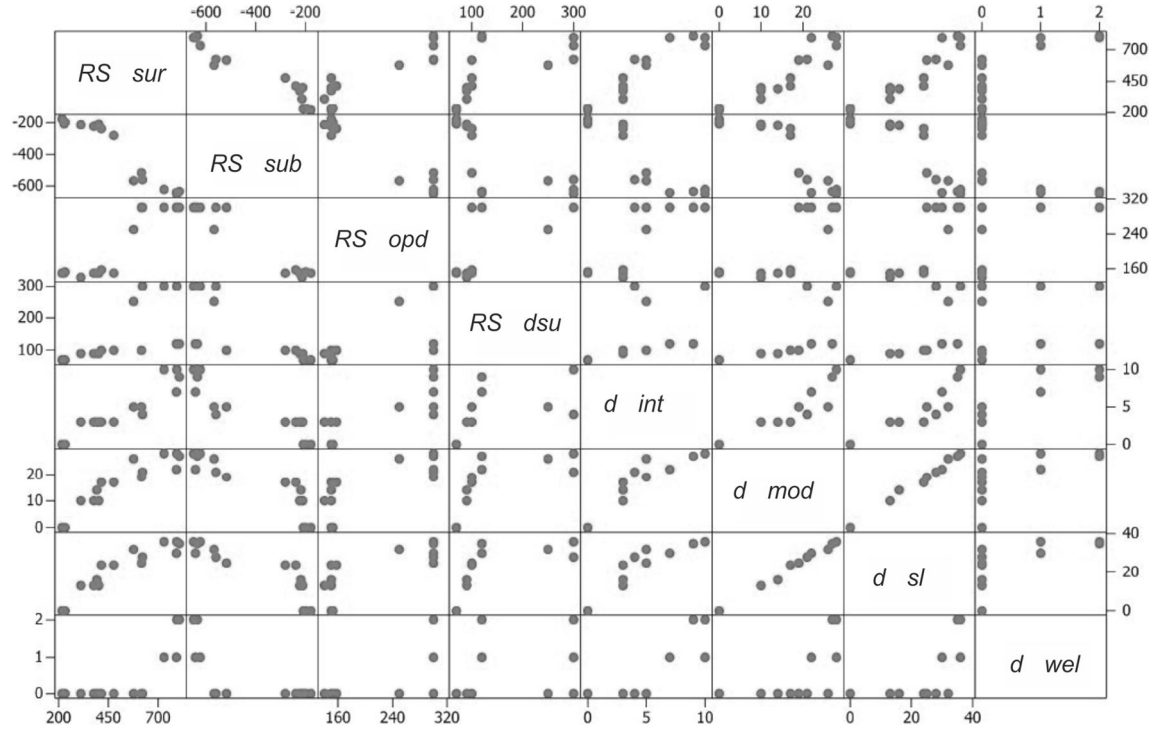

Fig. 15 Matrix plot illustrating correlations between residual stress and metallographic parameters during drilling

The correlation diagram in Fig. 17 illustrates the relationship between residual stress and metallographic parameters after operation of reaming.

Evaluation of the level of determination between the descriptive metallographic parameters and those of residual stress in operation of reaming outlined in Fig. 18 shows significant differences in between drilling. It is clear that the phenomenon of white etching layer cannot be explained by the regime of residual stress caused by the two-step hole-making process.

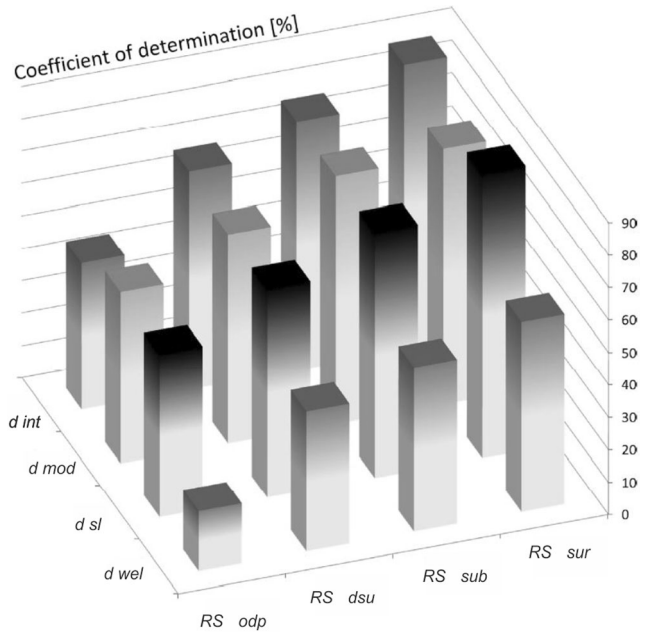

Fig. 16 Coefficients of determination: residual stress vs. metallographic parameters when drilling

When comparing results of d_{wel} data from roughing and finishing, it can be concluded that the tensile strain occurring on the surface RS_{sur} related to white layer formation is much higher in the case of drilling (RS_{sur} within the range of ~ 200–800 MPa) than during reaming operation (RS_{sur} at between ~ 100 and 350 MPa). However, the thickness of white layer during both machining processes was almost in the same range between 0 and ~ 2 μm. This phenomenon was described by Axinte and Andrews [30] in hole making by two-step machining process of RR1000 nickel-based superalloy. They observed that drilled holes and those finished with the normal reamer had a white layer on the machined surface. This is mainly due to the poor cutting performance of worn cutting edges of the normal reamer, which drags the material rather than shearing it. In addition, the material drags are likely to be generated by the cylindrical part of the cutting edges, where the depth of the cut is lower than the minimum chip thickness. Within proposed research was chip thickness during finishing operation equal to 150 μm (that is a radial depth of the cut) and the maximum tool wear for reaming was defined as VB_{max} = 150 μm. In contrast to drilling shown in Fig. 14, where intense residual stress on the surface RS_{sur} is accompanied by intense plastic deformation on the surface d_{int}, a subsequent finishing step generates a regime of residual stress, in which the subsurface residual stress RS_{sub} and the overall deformation depth of residual stress RS_{opd} are correlated best to the intense plastic

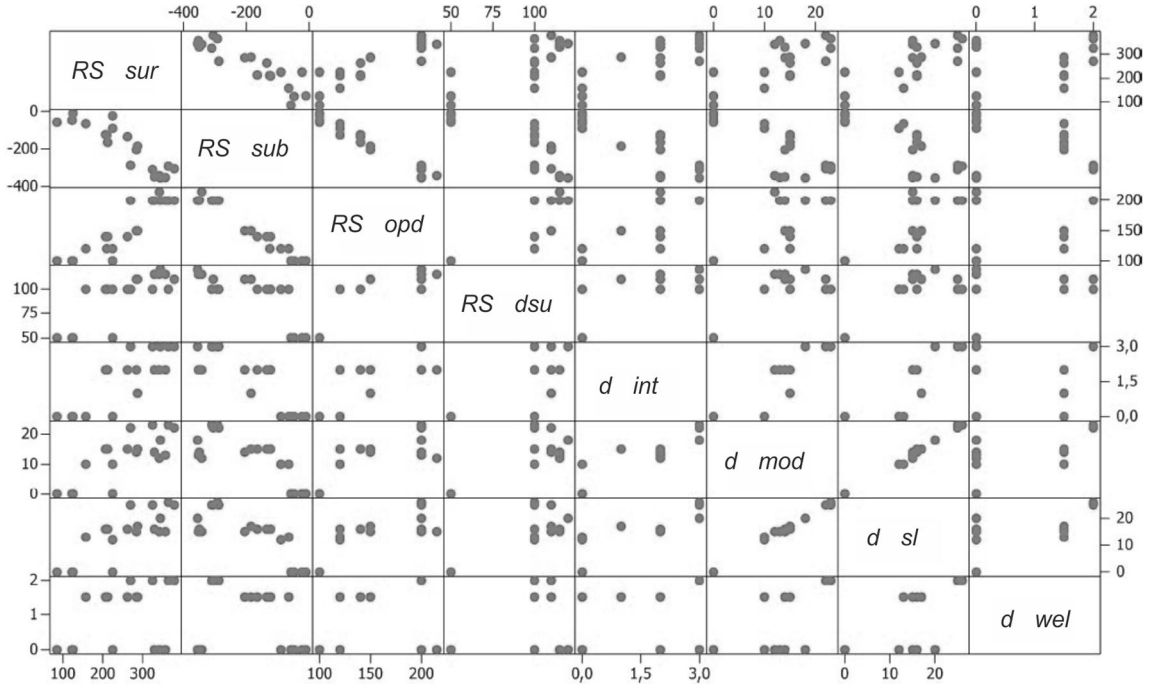

Fig. 17 Matrix plot illustrating correlations between residual stress and metallographic parameters when reaming

deformation on the surface d_{int}. To provide an initial explanation of this phenomenon, it may be useful to consider that the zone of plastic deformation right beneath the workpiece surface being generated by drilling is removed sequentially by reaming, thus leaving a significantly less deformed structure behind (it also depends on the workpiece allowance to be removed).

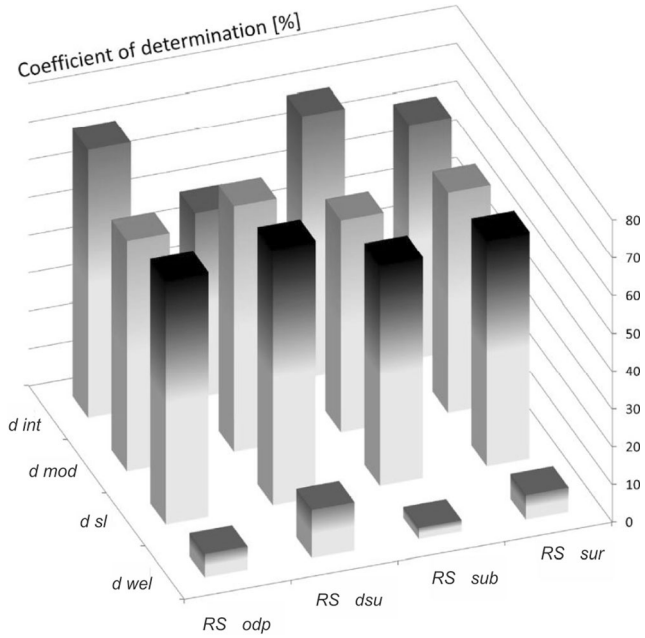

Fig. 18 Coefficients of determination: residual stress vs. metallographic parameters when reaming

4 Conclusions

Bolt holes machined in both drilled and drilled/finished conditions were investigated in terms of residual stress and metallography by employing their descriptive parameters. The evolution of these descriptive parameters near tool exit from the machined hole was tested in a considerable number of cutting tests using the verified regime of cutting tool and machining conditions. Possible correlations between metallography and residual stress indices were visualized by applying statistical methods. The results from metallography and from residual stress do not contradict themselves and indicate a capable cutting process that is performed within the specifications of engine makers. It appears as if the final status of residual stress in a finished hole cannot be independent from the formation of residual stress created by drilling. Overall, it can be stated that the experimental setup delivers reasonable results that reflect conditions complying with the manufacturing of highly stressed aero-engine components. The main results and conclusions of this paper are summarized below:

- In case of sharp tool edge during finishing operation, the maximum residual stress on the surface $RS_{sur} \approx 100$ MPa and in the subsurface $RS_{sub} \approx -200$ MPa is about half of that in drilling.
- The maximum penetration depth to subsurface $RS_{dsu} \approx 75$ μm in reaming with a new tool is slightly less compared to drilling (~ 25%). An increased tool wear, VB_{max}, makes this difference more significant.

- If was found that the occurrence of the white etching layer d_{wel} (in the range 0 to 2 μm) remains a random phenomenon that cannot be linked with any of the residual stress descriptive parameters especially in the case of finishing operation.
- Moreover, it can be concluded that RS_{sur}, especially in the case of drilling, is a powerful descriptive parameter within a dataset of RS evaluated in this work, carrying substantial information with respect to descriptive parameters of metallography under consideration.
- In addition, we have shown that in two-step manufacturing of bolt hole, the tool wear parameter VB_{max} can provide considerable information for the surface integrity regarding microstructure and residual stress state of highly stressed bolt holes in aircraft propulsion.
- It was found that considerations and results from drilling with twist drills can be transferred to very special drilling tools, the so-called face-cutting finishers that are used for the finishing operation of bolt holes. However, no available data were found for this tool-material combination as yet.

Acknowledgements This work was supported by the projects VEGA 1/0219/18: Development of intelligent monitoring system for zero-defect production of irreplaceable parts and VEGA 1/0434/15: Research on process dependent interface when milling with small diameter of end mill cutters. The authors wish to thank the Faculty of Mechanical Engineering of TU in Košice for the materials and financial support within the project development of the intelligent monitoring system for zero defect production. Finally, the authors would like to express their gratitude to Josef Beňo, PhD for his valuable comments and suggestions to improve the quality of this manuscript.

References

1. Madariaga A, Esnaola JA, Fernandez E, Arrazola PJ, Garay A, Morel F (2014) Analysis of residual stress and work-hardened profiles on Inconel 718 when face turning with large-nose radius tools. I nt J Adv Manuf Technol 71:1587–1598
2. Herbert CRJ, Kwong J, Kong MC, Axinte DA, Hardy MC, Withers PJ (2012) An evaluation of the evolution of workpiece surface integrity in hole making operations for a nickel-based superalloy. J Mater Process Technol 212:1723–1730
3. Renand X, Liu Z (2016) Influence of cutting parameters on work hardening behavior of surface layer during turning superalloy Inconel 718. Int J Adv Manuf Technol 86:2319–2327
4. Oliveira GP, Fonseca MC, Araujo AC (2017) Analysis of residual stress and cutting force in end milling of Inconel 718 using conventional flood cooling and minimum quantity lubrication. Int J Adv Manuf Technol 92:3265–3272
5. Chamanfara A, Monajatia H, Rosenbauma A, Jahazia M, Bonadarb A, Morinb E (2017) Microstructure and mechanical properties of surface and subsurface layers in broached and shot-peened Inconel-718 gas turbine disc fir-trees. Mater Charact 132:53–68
6. Chen YC, Liao YS (2003) Study on wear mechanisms in drilling of Inconel 718 superalloy, Dept. of Mechanical Engineering. National Taiwan University, Taipei
7. Ezugwu EO, Wang ZM, Okeke CI (1999) Tool life and surface integrity when machining Inconel 718 with PVD and CVD coated tools. Tribol Trans 42(2):353–360
8. Eckstein M, Mankova I (2012) Monitoring of drilling process for highly stressed aeroengine components. 5th CIRP Conference on High Performance Cutting, Procedia CIRP 1:587–592
9. Sharman ARC, Amarasinghe A, Ridgway K (2008) Tool life and surface integrity aspects when drilling and hole making in Inconel 718. J Mater Process Technol 200:424–432
10. Eckstein M (2004) Process Monitoring-ein innovativer Ansatz zur Steigerung der Zuverlässigkeit höchstbelasteter Bauteile der Fluggasturbine, Deutscher Luft- u. Raumfahrtkongress, Jahrbuch 2004
11. Champoux RL, Underwood JH, Kapp JA (1988) Analytical and experimental methods for residual stress effects in fatigue, ASTM, Philadelphia
12. Ehlers M, Müller H, Lohe D (1997) Simulation of stresses and residual stresses due to immersion cooling of tempering steel, ICRS-5, Linkoping/Sweden, p 400–405
13. Yu HJ, Schröder P, Besserdich A (1996) Zur Modellierung und Simulation der Wärmebehandlung metallischer Werkstoffe, HTM 51:48–51
14. Kleiner M, Kopp R, Homberg W (2004) Analysis of residual stresses in high pressure metal forming. Ann CIRP 53:211–214
15. Adam P (1998) Fertigungsverfahren von Turboflugtriebwerken. Birkhäuser Verlag, Basel
16. Adam P, Eckstein M (1992) Zeitfestigkeit und Randschicht-Eigenschaften durch Zerspanung bei Nickellegierungen, Materialwissenschaft. u. Werkstofftechnik 27:272–279
17. Liu CR (2002) A novel single-step superfinish hole-making process for maximum fatigue life. Research project abstract
18. Eckstein M (2007) Untersuchungen zur Intagritat gehonter Bolzenbohrungen in hochbelasteten Bauelementen der Fluggasturbine. In: Hoffmeister HW, Denkena B (ed) Jahrbuch Schleifen, Honen, Lappen und Polieren, Vulkan-Verlag GmbH, Essen, pp 319–328
19. Wessels T (2007) Bohren in Titan- und Nickelbasislegierungen, Dissertation. TU Braunschweig, Schriftenreihe des IWF, Vulkan Verlag
20. Farid AA, Sharif S, Nazami H (2009) Effect of machining parameters and cutting edge geometry on surface integrity when drilling and hole making in Inconel 718. SAE Int. J Mater Manuf 2:564–569
21. Osterle W, Li PX, Nolze G (1999) Influence of surface finishing on residual stress depth profiles of a coarse-grained nickel-based superalloy. Mater Sci Eng A 262:308–311
22. Kwong J, Axinte DA, Withers PJ (2009) The sensitivity of Ni-based superalloy to hole making operations: influence of process parameters on subsurface damage and residual stress. J Mater Process Technol 209:3968–3977
23. Ucak N, Cicek A (2018) The effect of cutting conditions on cutting temperature and hole quality in drilling of Inconel 718 using solid carbide drills. J Manuf Process 31:662–673
24. Beer N, Ozkaya E, Biermann D (2014) Drilling of Inconel 718 with geometry-modified twist drills. Procedia CIRP 24:49–55
25. Herbert CRJ, Axinte DA, Hardy MC, Brown PD (2011) Investigation into the characteristics of white layers produced in a nickel-based superalloy from drilling operations. Procedia Eng 19: 138–141
26. Dutilh V, Dessein G, Alexis J, Perrin G (2010) Links between machining parameters and surface integrity in drilling Ni-superalloys. Adv Mater Res 112:171–178
27. NN (2007) Metallography principles and procedures. LECO Corporation, St. Joseph

28. Schatt W, Worch H (1996) Werkstoffwissenschaft. 8th edn. Wiley-VCH, Weinheim
29. Sharman ARC, Hughes JI, Ridgway K (2004) Workpiece surface integrity and tool life issues when turning Inconel 718™ nickel based superalloy. Mach Sci Technol Int J 8(3):399–414
30. Axinte DA, Andrews P (2006) Some considerations on tool wear and workpiece surface quality of holes finished by reaming or milling in a nickel base superalloy. Proc Inst Mech Eng B J Eng Manuf 221:591–603
31. Sharman ARC, Hughes JI, Ridgway K (2015) The effect of tool nose radius on surface integrity and residual stresses when turning Inconel 718 TM. J Mater Process Technol 216:123–132
32. Sharman ARC, Hughes JI, Ridgway K (2006) An analysis of the residual stresses generated in Inconel 718TM when turning. J Mater Process Technol 173:359–367
33. Hood R, Soo SL, Aspinwall DK, Andrews P, Sage C (2011) Twist drilling of Haynes 282 superalloy, 1st CIRP Conference on Surface Integrity. Procedia Eng 19:150–155

Publisher's Note